

## MODELLING OF THIN LAYER SOLAR DRYING KINETICS AND EFFECTIVE DIFFUSIVITY OF *Urtica dioica* LEAVES

A. LAMHARRAR<sup>\*</sup>, A. IDLIMAM, A. ALOUANI, M. KOUHILA

Laboratory of Solar Energy and Medicinal Plants, Teacher's Training College,  
Cadi Ayyad University, BP 2400 Marrakesh, Morocco

<sup>\*</sup>Corresponding author: alamharrar@yahoo.fr

### Abstract

*Urtica dioica* is an endemic plant of Morocco used for its virtues in traditional medicine. The drying kinetics of *Urtica dioica* leaves in a convective solar dryer was studied. The kinetics of drying is studied for three temperatures (40, 50 and 60 °C), ambient air temperature ranged from 30 to 35 °C. The experimental results are used to determine the characteristic drying curve. Nine mathematical models have been used for the description of the drying curve. The Midilli-Kuck model was found to be the most suitable for describing the drying curves of *Urtica dioica* leaves. The drying parameters in this model were quantified as a function of the drying air temperature. Moisture transfer from *Urtica dioica* leaves was described by applying the Fick's diffusion model. Effective moisture diffusivity of the product was in the range of  $9.38 - 72.92 \times 10^{-11} \text{ m}^2/\text{s}$ . A value of 88,49 kJ/mol was determined as activation energy.

Keywords: Forced convection, Drying kinetics, *Urtica dioica*, Effective diffusivity, Activation energy.

### 1. Introduction

The medicinal and aromatic plants have a great importance for both the pharmaceutical industry and the traditional use. Solar drying is essential for preserving agricultural products, so it is necessary to know the drying process and storage of *Urtica dioica* leaves. The stability of a dehydrated medicinal plant is influenced by its water activity. *Urtica dioica* is known as nettle in Morocco Its root and leaf, which contain active pharmacologic compounds influencing cytological and physiological processes in the body, are used for medical purposes [1].

This plant had been used as a diuretic and as a mean of treating Arthritis and

**Nomenclatures**

$a, b, c,$	Model coefficients
$g, k, k_0,$	
$k_1, n$	
$D_{eff}$	Effective diffusivity, $m^2/s$
$D_v$	Drying air flow rate ( $m^2/s$ )
$E_a$	Activation energy (kJ/mol)
$f$	Dimensionless drying rate (-)
$L$	Half thickness (m)
$N$	Number of observations
$r$	Correlation coefficient
$R$	Universal gas constant (8.3145 J/mol.K)
$Sr$	Standard error
$t$	Drying time (min)
$T$	Absolute temperature (K)
$X$	Moisture content (% d.b)
$X_0$	Initial moisture content (% d.b)
$X_{eq}$	Equilibrium moisture content (% d.b)
$X_f$	Final moisture content (% d.b)
$X^*$	Moisture ratio (-)

**Greek Symbols**

$\theta$	Temperature ( $^{\circ}C$ )
$\chi^2$	Reduced chi-square

**Abbreviations**

CDC	Characteristic Drying Curve
DB	Dry basis
EXP	Experimental
PRE	Predicted

rheumatic diseases in the past [2]. The solar drying is essential for preserving the agricultural products. Then, it would be necessary to know the process of drying and storage for *Urtica dioica* leaves. The use of solar energy for drying various products has received considerable attention since food drying has a great effect on the quality of the dried products. Enclosed solar dryers have many advantages, as longer shelf life, product diversity and lighter weight for transportation and smaller space for storage. This could be expanded further with improvements in product quality and process applications. These solar dryers are essentially used in order to improve the quality. Simulation models are needed in the design of solar dryers. Several number of computer modelling programs have been developed to simulate the performance of solar drying systems [3].

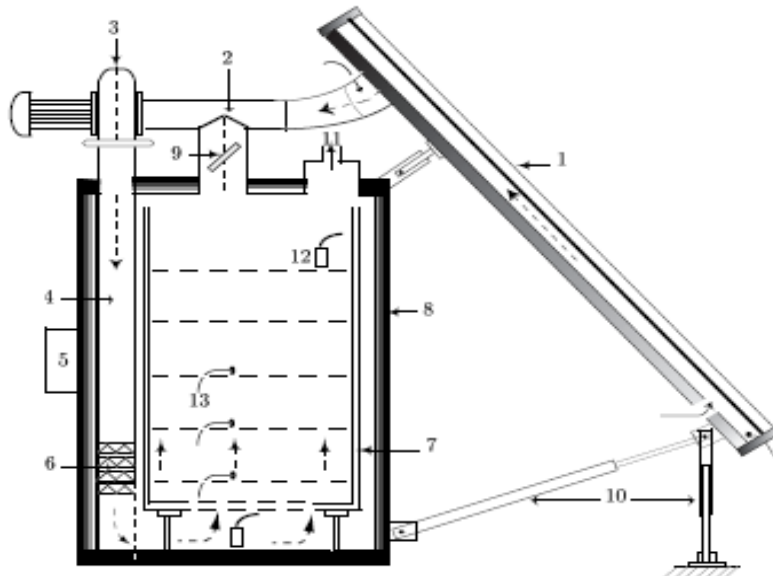
This study was mainly concerned with the:

- Determination of the effect of drying air temperature and air flow rate on the drying kinetics of *Urtica dioica* leaves.
- Fitting of the drying curves with nine mathematical models and determination of the characteristic drying curve (CDC).
- Calculation of effective diffusivity and the activation energy of *Urtica dioica* leaves.

## 2. Materials and Method

### 2.1. Drying experiments

The experimental apparatus consists of an indirect forced convection solar dryer with a solar air collector, an auxiliary heater, a circulation fan and a drying cabinet as shown in Fig. 1. A centrifugal fan (0.084 m<sup>3</sup>/s; 80 mm EC; 220 V, 0.1 kW), allows a theoretical velocity of 1.7 m/s, with a regulator which allows to fixed the air flow rate to 0.084 m<sup>3</sup>/s. It was described in detail in references [4, 5].



(1) solar collector, (2) ventilation duct, (3) fan, (4) suction line, (5) control box, (6) power supply, (7) floors, (8) drying cabinet, (9) air valve, (10) air inlet, (11) air outlet, (12) humidity probe, (13) thermocouple.



**Fig. 1. Partially solar dryer for medicinal plants.**

## 2.2. Experimental procedure

The *Urtica dioica* leaves used in the drying experiments was grown in Marrakech, Morocco. The mass of product used in drying experiments was  $(20 \pm 0.1)$  g by tray. However, the samples were uniformly spread evenly on a drying tray that was then placed on the first shelf of the drying cabinet. The heated air enters the drying cabinet below the trays and flows upwards through the samples. The relative humidities were measured by capacitance sensors. These values were determined by probes Humicolor  $\pm 2\%$ . A digital weighing apparatus ( $\pm 0.001$  g) measures the mass loss of the product during the drying process. During each drying experiment, the weight of the product on the tray was measured by removing it from the drying cabinet for approximately 15-20 seconds. These measurements were conducted each 10 min at the beginning of the experiment and 60 min in the end.

## 2.3. Moisture content and characteristic drying curves

For all the experiments conducted in the laboratory, drying *Urtica dioica* leaves is carried out in a solar dryer by setting the temperature, and following the evolution of the moist mass ( $M$ ) over time by successive weightings until it becomes stationary. This is followed by total dehydration of the product in an oven at  $105^\circ\text{C}$  for 24 h, in order to determine the dry mass ( $M_f$ ) of *Urtica dioica* leaves. Dry based moisture content at time ( $t$ ) is defined by Eq. (1).

$$X(t) = \frac{M - M_f}{M_f} \quad (1)$$

The final water content is a characteristic of each product. This is the optimal value for which the product does not deteriorate and retains its nutritional and organoleptic qualities (form, texture, color, odor and essential oils) [6, 7].

The Van Meel transformation [8] is applied for determining the characteristic drying curve of *Urtica dioica* leaves, using simply the initial moisture content  $X_0$  and the equilibrium moisture content  $X_{eq}$  derived from desorption data to obtain dimensionless moisture content and initial drying rate  $-(dX/dt)_0$  to normalize the drying rate as follows.

$$\begin{aligned} \text{In abscissa: } X \rightarrow X^* &= \frac{X - X_{eq}}{X_0 - X_{eq}} \quad 0 \leq X^* \leq 1 \\ \text{In ordinate: } \left( -\frac{dX}{dt} \right) \rightarrow f &= \frac{-\left( \frac{dX}{dt} \right)}{-\left( \frac{dX}{dt} \right)_0} \quad 0 \leq f \leq 1 \end{aligned} \quad (2)$$

## 2.4. Modelling drying curve

Modelling drying curves consist to develop a function verifying the equation:  $X^* = f(t)$  called drying characteristic equation. Several empirical or semi empirical models are used to describe the drying kinetics curves. The equations of these models expressing the evolution during the drying of the reduced moisture

content at any time of drying. These formulas contain constants that are adjusted to reconcile the theoretical predictions with experimental curves of drying.

In order to describe the drying speed of *Urtica dioica* leaves and to determine the most appropriate empirical equation, we used nine models of thin layer drying for medicinal plants which are grouped in Table 1.

Curves presenting the reduced moisture content depending on the drying time is described by the above nine models. The coefficients of each drying model were determined using the nonlinear optimization method based on the Levenberg-Marquard algorithm with Curve Expert 3.1 and Origin 6.1 software. The obtained solar drying curves were fitted with nine different thin-layer drying models (table 1) [9-16]. The correlation coefficient (*r*), the reduced chi-square ( $X^2$ ) were the statistical parameters used for selecting the best equation to describe the thin-layer drying curves of *Urtica dioica* leaves.

**Table 1. Selected mathematical models applied to the drying curves.**

Model name	Model equation
Newton	$X^* = \exp(-kt)$
Page	$X^* = \exp(-kt^n)$
Henderson and Pabis	$X^* = a \exp(-kt)$
Logarithmic	$X^* = a \exp(-kt) + c$
Two terms	$X^* = a \exp(-k_0t) + b \exp(-k_1t)$
Two term exponentials	$X^* = a \exp(-kt) + (1-a) \exp(-kat)$
Wang and Singh	$X^* = 1 + at + bt^2$
Approximation of diffusion	$X^* = a \exp(-kt) + (1-a) \exp(-kbt)$
Midilli-Kucuk	$X^* = a \exp(-kt^n) + bt$

For choosing the appropriate model for describing the allure of drying kinetics, we relying on the following criteria:

- (*r*) high correlation coefficient
- $X^2$  reduced minimum square

These statistical parameters are defined by Eq. (3):

$$\chi^2 = \frac{\sum_{i=1}^N (x_{pre,i}^* - x_{exp,i}^*)^2}{N - n} \tag{3}$$

where,

$\chi_{pre,i}^*$  :  $i^{eme}$  Moisture ratio predicted by model

$\chi_{exp,i}^*$  :  $i^{eme}$  Experimental moisture ratio

*N* : Number of experimental data

*n* : Number of variables in each model

### 3. Results and Discussion

The solar drying experiments were carried out during the period of April to Mai 2014 in Marrakesh, Morocco. During the experiments, ambient air temperature ranged from 30°C to 35°C, ambient air relative humidity from 23 to 35%, drying air temperature from 40 to 60 °C and drying air flow rate at 0.084 m<sup>3</sup>/s. The initial moisture content  $X_0$  of the *Urtica dioica* leaves ranged from 3.21 to 4.32 % db and was reduced to the final moisture content which varies from 0.11 to 0.17 % db (Table 2).

**Table 2. Drying conditions during experiments in the solar dryer of *Urtica dioica* leaves.**

EXP	Dy (m <sup>3</sup> /s)	$\theta \pm 0.1$ (°C)	Rh $\pm 2$ (%)	$X_0$	$X_f$ (% d.b)	t (min)
1	0.084	40.0	31	3.21	0.17	260
2	0.084	50.0	30	3.39	0.14	110
3	0.084	60.0	35	4.32	0.11	50

#### 3.1. Drying curves

The variation of moisture content versus drying time and the drying rate versus moisture content are given in Figs. 2 and 3 respectively. It is apparent that there is an absence of phase 0, the increasing drying rate period, where the temperature of the product is increased without any substantial loss of water and phase 1, the constant drying rate period. There is only the presence of the falling drying rate period (phase 2). These results are in agreement with the earlier observations [14- 18].

The drying air conditions have an important influence on the rates of these curves. At constant drying air flow rate (0.084 m<sup>3</sup>/s), the changes in the drying rate versus moisture content are shown in Fig. 3. It is apparent that the drying rate decreases continuously with decreasing moisture content. The drying rate increases with the increase of the drying air temperature and the highest values of drying rate were obtained in experiment for  $\theta = 60$  °C.

The *Urtica dioica* leaves, on average, have the following dimensions (4 cm x 1 cm). The fresh and dried product at 50 °C is shown in Fig. 4.

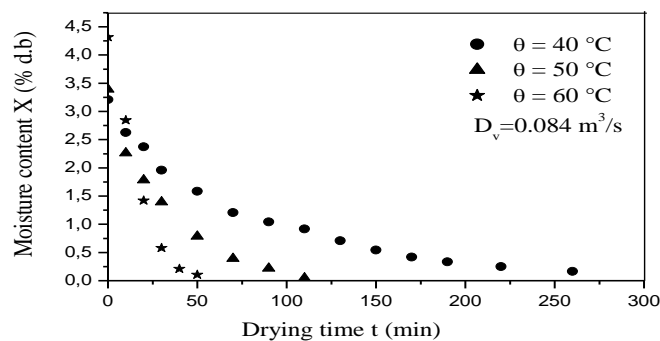


**Fig. 2. Variation of moisture content as a function of time for different drying air conditions of *Urtica dioica* leaves.**

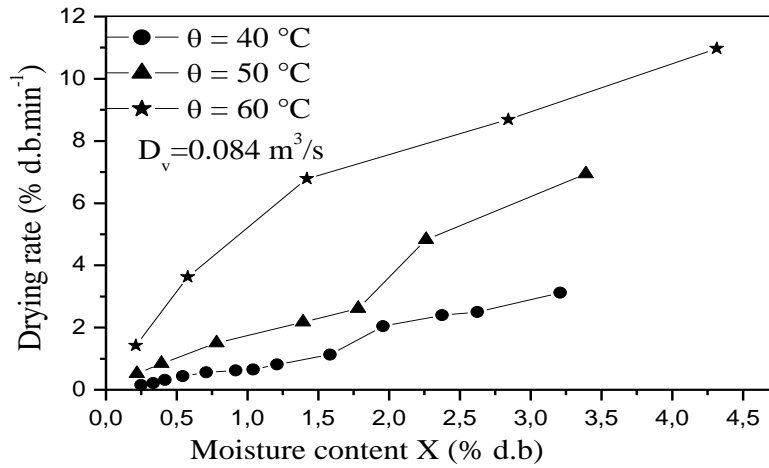


Fig. 3. Influence of drying air temperature on drying rate during drying of *Urtica dioica* leaves.



(a) *Urtica dioica* leaves fresh

(b) *Urtica dioica* leaves dried

Fig. 4. *Urtica dioica* leaves fresh and dried.

### 3.2. Characteristic drying curve

The change in the moisture ratio versus dimensionless drying rate  $f$  is given in Fig. 5, showing that all solar drying curves obtained for the different tested conditions, fall into a tight band, indicating that the effect of variation in different conditions is small over the range tested. A polynomial model was found the best to fit the dimensionless experimental data of the *Urtica dioica* leaves.

$$f = 1.006 X^* \tag{4}$$

The criteria used to evaluate goodness of fit was the standard error ( $S_r = 0.07$ ) and the correlation coefficient ( $r = 0.93$ ).

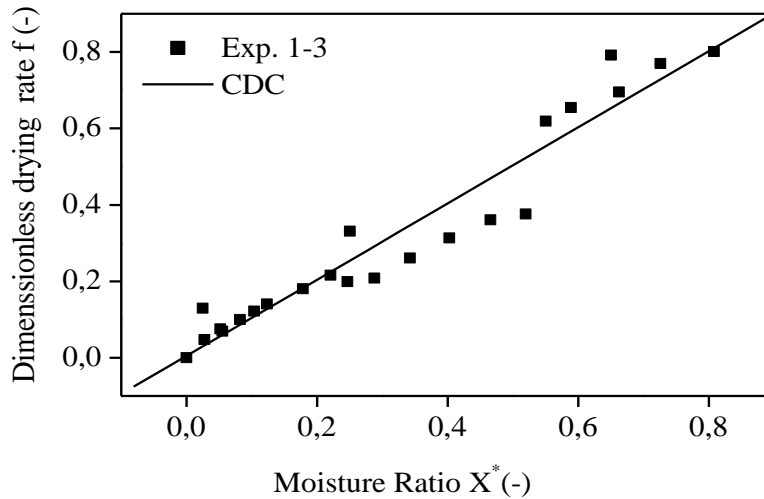


Fig. 5. Characteristic drying curve (CDC) of *Urtica dioica* leaves.

### 3.3. Fitting of the drying curves

The moisture content data at different drying air temperatures were converted to moisture ratio and then the curve fitting computations with the drying time carried on the nine drying models. The drying model coefficients were determined and presented in Table 3. It was assumed that the model, which has the highest ( $r$ ), lowest ( $X_2$ ) is the best suited one.

As shown in Table 3, the Midilli–Kucuk model is the appropriate for describing the thin layer drying curves of *Urtica dioica* leaves. The coefficients of the accepted model for thin layer forced solar drying of the *Urtica dioica* leaves were as Eq. (5):

$$X^* = a \exp(-kt^n) + bt \quad (5)$$

where,

$$a(\theta) = 1.0561 - 0.00229 \theta + 2.25 \cdot 10^{-5} \theta \quad (6)$$

$$k(\theta) = -0.8729 + 0.03823 \theta - 3.905 \cdot 10^{-4} \theta^2 \quad (7)$$

$$n(\theta) = 7.9469 - 0.3191 \theta + 0.00352 \theta^2 \quad (8)$$

$$b(\theta) = 0.0141 - 6 \cdot 10^{-4} \theta + 6 \cdot 10^{-6} \theta^2 \quad (9)$$

The four expressions, Eqs. (6) to (9), predicted well the moisture ratio at three drying temperatures 40, 50 and 60°C for the *Urtica dioica* leaves with an ( $r$ ) of 1 and  $S_r$  of 0.

**Table 3. Statistical parameters for each model according to the drying temperature.**

Model	$\theta(^{\circ}\text{C})$	Coefficients	$r$	$\chi^2$
Newton	40	$k = 1.48 \cdot 10^{-2}$	0.9958	$9 \cdot 10^{-4}$
	50	$k = 3.26 \cdot 10^{-2}$	0.9966	$9 \cdot 10^{-4}$
	60	$k = 0.06$	0.9874	$4 \cdot 10^{-3}$
Page	40	$k = 2.34 \cdot 10^{-2}; n = 0.89$	0.9976	$5 \cdot 10^{-4}$
	50	$k = 4.24 \cdot 10^{-2}; n = 0.93$	0.9974	$9 \cdot 10^{-4}$
	60	$k = 2.34 \cdot 10^{-2}; n = 0.89$	0.9998	$7.110 \cdot 10^{-5}$
Henderson et Pabis	40	$a = 0.96; k = 1.41 \cdot 10^{-2}$	0.997	$7 \cdot 10^{-4}$
	50	$a = 0.98; k = 3.17 \cdot 10^{-2}$	0.997	$9 \cdot 10^{-4}$
	60	$a = 1.04; k = 6.18 \cdot 10^{-2}$	0.9884	$4.6 \cdot 10^{-3}$
Logarithmic	40	$a = 0.96; k = 1.38 \cdot 10^{-2}; c = -6.7 \cdot 10^{-3}$	0.997	$7 \cdot 10^{-4}$
	50	$a = 0.99; k = 3.0110^{-2}; c = -1.78 \cdot 10^{-2}$	0.9972	$9 \cdot 10^{-4}$
	60	$a = 1.18; k = 4.41 \cdot 10^{-2}; c = -0.16$	0.9962	$2 \cdot 10^{-3}$
Two terms	40	$a = 0.91; k_0 = 1.33 \cdot 10^{-2}; b = 8.67 \cdot 10^{-2}; k_1 = 1.68 \cdot 10^{-1}$	0.9981	$5 \cdot 10^{-4}$
	50	$a = 0.71; k_0 = 3.25 \cdot 10^{-2}; b = 2.6810^{-1}; k_1 = 2.9510^{-2}$	0.997	$1.2 \cdot 10^{-3}$
	60	$a = 0.73; k_0 = 6.19 \cdot 10^{-2}; b = 3.04 \cdot 10^{-2}; k_1 = 6.15 \cdot 10^{-2}$	0.9884	0.0092
Two term exponentials	40	$a = 9.0210^{-2}; k = 1.4710^{-1}$	0.9981	$4 \cdot 10^{-4}$
	50	$a = 6.2710^{-1}; k = 3.910^{-2}$	0.9967	$9 \cdot 10^{-4}$
	60	$a = 2.08; k = 9.46 \cdot 10^{-2}$	0.9992	$3 \cdot 10^{-4}$
Wang et Singh	40	$a = -9.9 \cdot 10^{-3}; b = 2.4610^{-5}$	0.9721	$4 \cdot 10^{-4}$
	50	$a = -2.26 \cdot 10^{-2}; b = 1.2710^{-4}$	0.9796	$9 \cdot 10^{-4}$
	60	$a = -4.28 \cdot 10^{-2}; b = 4.5610^{-4}$	0.9991	$3 \cdot 10^{-3}$
Approximation de la diffusion	40	$a = 1.56; k = 1.48 \cdot 10^{-2}; b = 1.003$	0.9958	$1 \cdot 10^{-3}$
	50	$a = 1.65; k = 3.28 \cdot 10^{-2}; b = 1.013$	0.9966	$1.110 \cdot 10^{-3}$
	60	$a = 10.23; k = 2.76 \cdot 10^{-2}; b = 9.17 \cdot 10^{-1}$	0.9965	$1.8 \cdot 10^{-3}$
Midilli-Kucuk	40	$a = 1; k = 3.13 \cdot 10^{-2}; n = 8.0710^{-1}; b = -3 \cdot 10^{-4}$	<b>0.9990</b>	<b><math>3 \cdot 10^{-4}</math></b>
	50	$a = 9.98 \cdot 10^{-1}; k = 6.21 \cdot 10^{-2}; n = 7.79 \cdot 10^{-2}; b = -910^{-4}$	<b>0.9994</b>	<b><math>2 \cdot 10^{-4}</math></b>
	60	$a = 9.99 \cdot 10^{-1}; k = 1.48 \cdot 10^{-2}; n = 1.45; b = -3 \cdot 10^{-4}$	<b>0.9999</b>	<b><math>2.98 \cdot 10^{-5}</math></b>

### 3.4. Effective diffusivities

According to the experimental drying curves of *Urtica dioica* leaves, we note only a falling drying rate period and liquid diffusion controls process. Fick's second law can be used to describe drying behaviour. The solution of Fick's second law in

slab geometry was found from using the following expression (Eq. (10)), cited by Madamba et al. and Crank. [19, 20]:

$$X^* = \frac{8}{\pi^2} \sum_{n=0}^{\infty} \frac{1}{(2n+1)^2} \exp\left(-\frac{(2n+1)^2 \pi^2 D_{eff} t}{4L^2}\right) \quad (10)$$

For long drying periods Eq. (11) can be expressed in logarithmic form:

$$\ln(X^*) = \ln\left(\frac{8}{\pi^2}\right) - \left(\frac{\pi^2 D_{eff} t}{4L^2}\right) \quad (11)$$

where  $X^*$  is the moisture ratio.  $L$  is the half thickness of *Urtica dioica* leaves and  $D_{eff}$  is the effective diffusion coefficient of *Urtica dioica* leaves dried.

Effective diffusivity is also typically calculated by using slope of Eq. (12), namely when natural logarithm of  $X^*$  versus time was plotted. straight line with a slope was obtained:

$$\text{Slope} = \frac{\pi^2 D_{eff}}{4L^2} \quad (12)$$

The slope of Eq. 13 is the measure of the diffusivity. Figure 6 shows the plot of experimental results of  $\ln(X^*)$  versus drying time for the studied range of temperatures. It is apparent at constant drying air flow rate. That  $D_{eff}$  increases with the increase of drying air temperature (Table 4). These values are almost equal to the energy of activation of different products [21, 22].

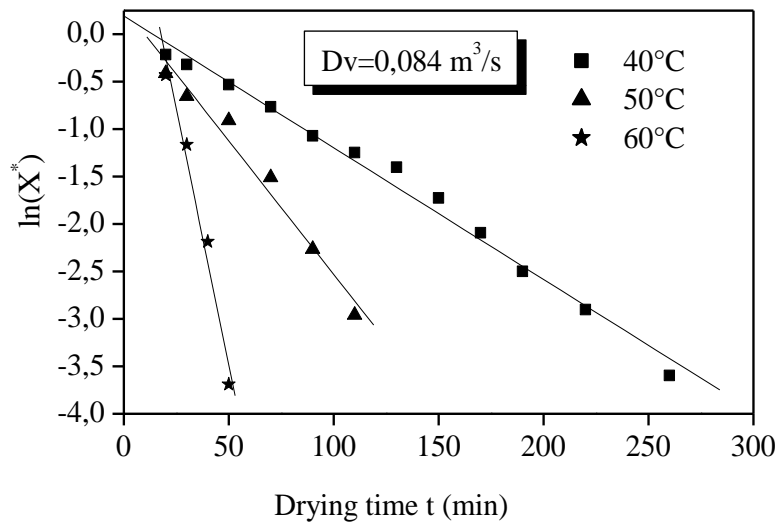


Fig. 6. Plot of  $\ln(X^*)$  vs. drying time for different drying air conditions.

**Table 4. Values of effective diffusivity of *Urtica dioica* leaves.**

Exp	Drying air flow (m <sup>3</sup> /s)	Temperature θ (°C)	$D_{eff}$ (m <sup>2</sup> /s)	(r)
1	0.084	40	9.382 10 <sup>-11</sup>	0.994
2	0.084	50	19.008 10 <sup>-11</sup>	0.987
3	0.084	60	72.924 10 <sup>-11</sup>	0.987

### 3.5. Activation energy

The activation energy in a drying process,  $E_a$ , is the minimum amount of energy which must be overcome for this process to occur. The origin of the self-diffusion is thermal agitation. Diffusion is thermally activated, and the diffusion coefficient follows an Arrhenius law.

The correlation between the drying conditions and the determined values of the effective diffusivity may be expressed by using an Arrhenius type equation [22] such as:

$$D_{eff} = D_0 \exp\left(-\frac{E_a}{RT}\right) \tag{13}$$

where  $D_0$  is the pre-exponential factor of the Arrhenius equation (m<sup>2</sup>/s).  $E_a$  is the activation energy of the moisture diffusion (kJ/mol). T is the air temperature absolute and R is the universal gas constant (J/mol.K).

The activation energy ( $E_a$ ) was calculated from the slope of the plot on  $\ln(D_{eff})$  versus reciprocal of the absolute temperature as presented in Fig. 7. The activation energy of *Urtica dioica* leaves was found to be 88.49kJ/mol.

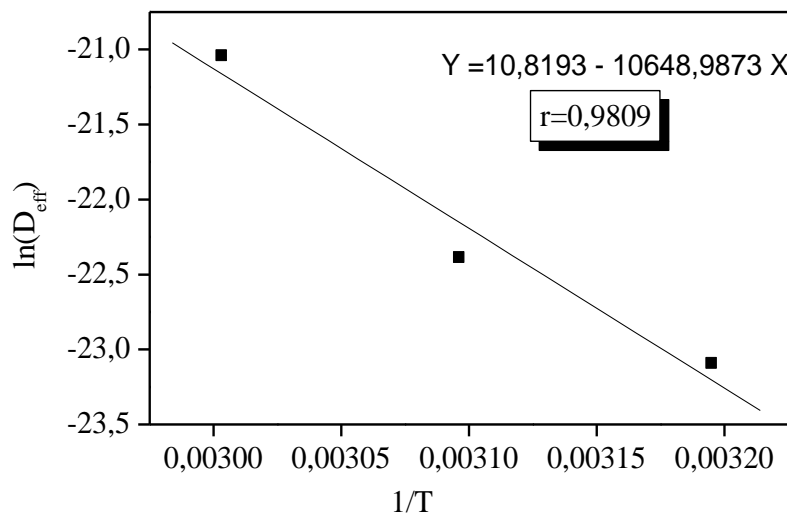


**Fig. 7. Influence of drying air temperature on the effective diffusivity.**

#### 4. Conclusion

The drying rate of *Urtica dioica* leaves in an indirect forced convection solar dryer has been determined. The obtained results show that the main factor influencing the drying kinetics was the drying air temperature. These results have been exploited to determine the characteristic drying curve, which is important to accurate information about the drying rate of *Urtica dioica* leaves.

Nine different mathematical models were tested to fit the experimental data of thin layer drying of *Urtica dioica* leaves. the Midilli-Kucuk drying model was the most suitable to describing the solar drying curves of *Urtica dioica* leaves with a correlation coefficient ( $r$ ) of 0.9999 and  $X^2$  of  $2.98 \times 10^{-5}$ . The drying parameters  $a$ ,  $k$ ,  $n$  and  $b$  in Midilli-Kucuk's equation can be expressed as a linear function of the temperature with an  $r$  of 1 and  $S_r$  of 0. The effective diffusivity values changed from  $9.38 \times 10^{-11}$  to  $72.92 \times 10^{-11}$  m<sup>2</sup>/s within the given temperature range and increased as temperature increases. An Arrhenius relation with an activation energy value of 88.49 kJ/mol expressed the effect of temperature on the effective diffusivity.

#### References

1. Krystofova, O.; Adam, V.; Babula, P.; Zehnalek, J.; Beklova, M.; Havel, L.; and Kizek, R. (2010). Effects of various doses of selenite on stinging nettle (*Urtica dioica* L.). *International Journal of Environmental Research and Public Health*, 7, 3804-3815.
2. Bellakhdar, J. (1997). *La Pharmacopée marocaine traditionnelle. Médecine arabe ancienne et savoirs populaires*. Paris: Ibis Press.
3. Midilli, A.; and Kucuk, H. (2003). Mathematical modeling of thin layer drying of pistachio by using solar. *Energy Conversion and Management*, 44(7), 1111-1122.
4. Ait Mohamed, L.; Kouhila, M.; Jamali, A.; Lahsasni, S.; Kechaou, N.; and Mahrouz, M. (2005). Single layer solar drying behaviour of Citrus aurantium leaves under forced convection. *Energy Conversion and Management*, 46(9-10), 1473-1483.
5. Lahsasni, S.; Kouhila, M.; Mahrouz, M.; and Jaouhari, J. T. (2004). Drying kinetics of prickly pear fruit (*Opuntia ficus indica*). *Journal of Food Engineering*, 61(2), 173-179.
6. Verma, L.R.; Bucklin, R.A.; Endan, J.B.; and Wratten, F.T. (1985). Effects of drying air parameters on rice drying models. *Transactions of the American Society of Agricultural Engineers*, 28(1), 296-301.
7. Karathanos, V.T. (1999). Determination of water content of dried fruits by drying kinetics. *Journal of Food Engineering*, 39(1), 337-344.
8. Van Mee, D.A. (1958). Adiabatic convection batch drying with recirculation of air. *Chemical Engineering Science*, 9(1), 36-44.
9. Bruce, D.M. (1985). Exposed layer barley drying: three models fitted to new data up to 150 °C. *Journal of Agricultural Engineering Research*, 32, 337-347.

10. Doymaz, I. (2007). The kinetics of forced convective air-drying of pumpkin slices. *Journal of Food Engineering*, 79(1), 243-248.
11. Henderson, S.M.; and Pabis, S. (1961). Grain drying theory. I. Temperature effects on drying coefficient. *Journal of Agricultural Engineering Research*, 6(1), 169-174.
12. Togrul, T.I.; and Pehlivan, D. (2003). Modelling of drying kinetics of single apricot. *Journal of Food Engineering*, 58(1), 23-32.
13. Henderson, S.M. (1974). Progress in developing the thin layer drying equation. *Transactions of the American Society of Agricultural Engineers*, 17(1), 1167-1168.
14. Sharaf-Elden, Y.I.; Blaisdell, J.L.; and Hamdy, M.Y.A. (1980). A model for ear corn drying. *Transactions of the American Society of Agricultural Engineers*, 23(1), 1261-1265.
15. Wang, C.Y.; and Singh, R.P. (1978). Use of variable equilibrium moisture content in modelling rice drying. *Transactions of the ASAE (American Society of Agricultural Engineers)*, 11(1), 668-672.
16. Yaldiz, O.; Ertekin, C.; and Uzun, H. I. (2001). Mathematical modelling of thin layer solar drying of sultana grapes. *Energy*, 26(5), 457-465.
17. Sobral, P.A.; Lebert, A.; and Bimbenet, J.J. (1999). Isothermes de désorption de la pomme de terre entre 40 et 70°C. *Science Des Aliments*, 19(1), 711-720.
18. Mohanraj, M.; and Chandrasekar, P. (2009). Performance a forced convection solar drier integrated with gravel as heat storage material for Chili drying. *Journal of Engineering Science and Technology*, 4(3), 305-314.
19. Madamba, P.S.; Driscoll, R.H.; and Buckle, K.A. (1996). The thin layer drying characteristics of garlic slices. *Journal of Food Engineering*, 29(1), 75-97.
20. Crank, J. (1975). *Mathematics of diffusions* (2<sup>nd</sup> ed.). London: Oxford University Press.
21. Kara, C.; and Doymaz, I. (2015). Thin layer drying kinetics of by-products from pomegranate juice processing. *Journal of Food Processing and Preservation*, 39(5), 480-487.
22. Hii, C.L; and Ogugo, J.F. (2014). Effect of pre-treatment on the drying kinetics and product quality of star fruit slices. *Journal of Engineering Science and Technology*, 9(1), 123-125.